Electronic Supplementary Information

Experimental section

Materials: Sodium nitrate ($NaNO_3$, 99.0%), sodium nitrite ($NaNO_2$, 99.0%), ammonium chloride (NH_4Cl), sodium hydroxide (NaOH), sodium sulfate (Na_2SO_4), sodium salicylate ($C_7H_5NaO_3$), trisodium citrate dihydrate ($C_6H_5Na_3O_7{\cdot}2H_2O$), p–dimethylaminobenzaldehyde ($C_9H_{11}NO$), sodium nitroferricyanide dihydrate ($C_5FeN_6Na_2O{\cdot}2H_2O$), 0.8 wt% sulfamic acid solution (H_3NO_3S), sodium dihydrogen phosphate dihydrate (NaH_2PO_4), disodium hydrogen phosphate dodecahydrate (Na_2HPO_4) and sodium hypochlorite solution (NaClO) were purchased from Aladdin Ltd. (Shanghai, China). Iron nitrate nonahydrate ($Fe(NO_3)_3{\cdot}9H_2O$), Cobalt nitrate hexahydrate ($Co(NO_3)_2{\cdot}6H_2O$), urea and ammonium fluoride (NH_4F) were purchased from Chengdu Kelong Chemical Regent Co. Ltd. Sulfuric acid (H_2SO_4), hydrogen peroxide (H_2O_2), hydrochloric acid (HCl), hydrazine monohydrate ($N_2H_4{\cdot}H_2O$) and ethylalcohol (C_2H_5OH) were bought from Beijing Chemical Corporation. (China). chemical Ltd. in Chengdu. Carbon cloth (CC) was purchased from Qingyuan Metal Materials Co., Ltd (Xingtai, China). All reagents used in this work were analytical grade without further purification.

Preparation of $FeCo_2O_4$/CC and Co_3O_4/CC: All the chemicals in this work were of analytical grade and directly used after purchase without further purification. $FeCo_2O_4$ nanowire grown on CC was prepared as following. In a typical procedure, 1 mmol of $Fe(NO_3)_3{\cdot}9H_2O$, 2 mmol of $Co(NO_3)_2{\cdot}6H_2O$, 4 mmol of NH_4F and 10 mmol of urea were dissolved in 35 mL deionized water under violent stirring for 20 min at room temperature. A piece of CC (1 × 4 cm) was immersed with concentrated HNO_3 solution for 2 h, and then cleaned with acetone, ethanol and deionized water for 10 min each. The solution was transferred into a 40 mL Teflon-lined autoclave and the cleaned CC substrate was immersed into the solution. The autoclave was sealed and maintained at 120 ˚C for 6 h. After the autoclave cooling to room temperature naturally, as-obtained precursor was taken out, washed with ethanol and distilled water for several times, and dried at 70 ˚C for 2 h. Finally, the precursor was put in a muffle furnace and annealed at 400 ˚C in air for 2 h to obtain $FeCo_2O_4$ nanowire

supported on CC. Co_3O_4/CC as one control catalyst was also prepared under otherwise identical conditions used for preparing $FeCo_2O_4$/CC expect without adding Fe salt in the hydrothermal process.

Preparation of Fe_2O_3/CC: Fe_2O_3/CC was prepared as follows. 0.6 g $Fe(NO_3)_3 \cdot 9H_2O$ and 0.24 g Na_2SO_4 was diluted into 35 mL aqueous solution. Then the solution was transferred into a Teflon-lined stainless autoclave (50 mL), and a piece of CC (1 cm × 4 cm) was immersed into the autoclave contained solution. The autoclave was sealed and maintained at 120 °C for 6 h in an electric oven. After the autoclave cooled down naturally to room temperature, the Fe_2O_3/CC was obtained after annealing in Ar gas at 450 ºC for 3 h.

Characterizations: XRD data were acquired by a LabX XRD–6100 X-ray diffractometer with a Cu Kα radiation (40 kV, 30 mA) of wavelength 0.154 nm (SHIMADZU, Japan). SEM measurements were carried out on a GeminiSEM 300 scanning electron microscope (ZEISS, Germany) at an accelerating voltage of 5 kV. XPS measurements were performed on an ESCALABMK II X-ray photoelectron spectrometer using Mg as the exciting source. The absorbance data of spectrophotometer was measured on UV-Vis spectrophotometer. TEM image was obtained from a Zeiss Libra 200FE transmission electron microscope operated at 200 kV.

Electrochemical measurements: All electrochemical measurements were performed in a two-compartment cell separated by a treated Nafion 117 membrane using the CHI660E electrochemical workstation (Shanghai, Chenhua) with a standard three–electrode setup. Electrolyte solution was Ar-saturated 0.1 M NaOH with 20 mM NO_3^-, using $FeCo_2O_4$/CC (1.0 × 0.5 cm^2) as the working electrode, a carbon rod as the counter electrode, and a Hg/HgO as the reference electrode. All the potentials reported in our work were converted to reversible hydrogen electrode (RHE) scale via calibration with the following equation: E (RHE) = E (vs. Hg/HgO) + 0.0591 × pH + 0.098 V and the current density was normalized by the geometric surface area.

Determination of NH_3: Concentration of produced NH_3 was determined by spectrophotometry measurement with indophenol blue method (the obtained

electrolyte was diluted 40 times).[1] In detail, 2 mL of the diluted catholyte was obtained from the cathodic chamber and mixed with 2 mL of a 1 M NaOH solution that contained salicylic acid and sodium citrate. Then, 1 mL of 0.05 M NaClO and 0.2 mL of 1 wt% $C_5FeN_6Na_2O$ were dropped in the collected electrolyte solution. After standing at room temperature for 2 h, the ultraviolet-visible absorption spectrum was measured. The concentration-absorbance curve was calibrated using the standard NH_4Cl solution with NH_3 concentrations of 0, 0.2, 0.5, 1.0, 2.0 and 5.0 μg mL^{-1} in 0.1 M NaOH. The absorbance at 655 nm was measured to quantify the NH_3 concentration using standard NH_4Cl solutions ($y = 0.4407x + 0.0318$, $R^2 = 0.9999$).

Determination of NO_3^-: Firstly, 0.05 mL electrolyte was taken out from the electrolytic cell and diluted to 5 mL to detection range. Then, 0.1 mL 1 M HCl and 0.01 mL 0.8 wt% H_3NO_3S solution were added into the aforementioned solution. After 15 minutes, the absorbance was detected by UV-Vis spectrophotometry at a wavelength of 220 nm and 275 nm. The final absorbance of NO_3^- was calculated based on the following equation: $A=A_{220nm} - 2A_{275nm}$. The calibration curve can be obtained through different concentrations of $NaNO_3$ solutions and the corresponding absorbance. The fitting curve ($y = 0.05549x - 0.00442$, $R^2 = 0.9993$) shows good linear relation of absorbance value with NO_3^- concentration.

Determination of NO_2^-: Owing to the large concentration of solution, the obtained reaction solutions were diluted 5 times. The NO_2^- concentration was analyzed using the Griess test.[2] The Griess reagent was prepared by dissolving 0.1 g N–(1–naphthyl) ethylenediamine dihydrochloride, 1.0 g sulfonamide and 2.94 mL H_3PO_4 in 50 mL deionized water. In a typical colorimetric assay, the 1.0 mL Griess reagent was mixed with the 1.0 mL nitrite-containing solution and 2.0 mL H_2O and allowed to react at room temperature for 10 min, in which sulfonamide reacts with NO_2^- to form a diazonium salt and then further reacts with amine to form an azo dye (magenta). The absorbance at 540 nm was measured to quantify the NO_2^- concentration with a standard curve of NO_2^- ($y = 0.22194x + 0.03249$, $R^2 = 0.9998$).

Determination of N_2H_4: In this work, we used the method of Watt and Chrisp[2] to determine the concentration of produced N_2H_4. The chromogenic reagent was a mixed

solution of 5.99 g $C_9H_{11}NO$, 30 mL HCl and 300 mL C_2H_5OH. In detail, 1 mL electrolyte was added into 1 mL prepared color reagent and stirred for 15 min in the dark. The absorbance at 455 nm was measured to quantify the N_2H_4 concentration with a standard curve of hydrazine ($y = 0.6871x + 0.10688$, $R^2 = 0.9998$).

Calculations of FE, NH_3 yield, selectivity and conversion rate:

$$FE = (8 \times F \times [NH_3] \times V) / (M_{NH_3} \times Q) \times 100\%$$

$$NH_3 \text{ yield} = ([NH_3] \times V) / ((M_{NH_3} \times t \times A)$$

$$\text{Selectivity} = [NH_3] / \Delta[NO_3^-] \times 100\%$$

$$\text{Conversion rate} = \Delta[NO_3^-] / [NO_3^-] \times 100\%$$

Where F is the Faradic constant (96485 C mol^{-1}), $[NH_3]$ is the measured NH_3 concentration, V is the volume of electrolyte in the anode compartment (70 mL), M_{NH_3} is the molar mass of NH_3, Q is the total quantity of applied electricity, t is the electrolysis time, A is the loaded area of catalyst (1.0 × 0.5 cm^2), $[NO_3^-]$ is the initial concentration of NO_3^- and $\Delta[NO_3^-]$ is the concentration difference of NO_3^- before and after electrolysis.

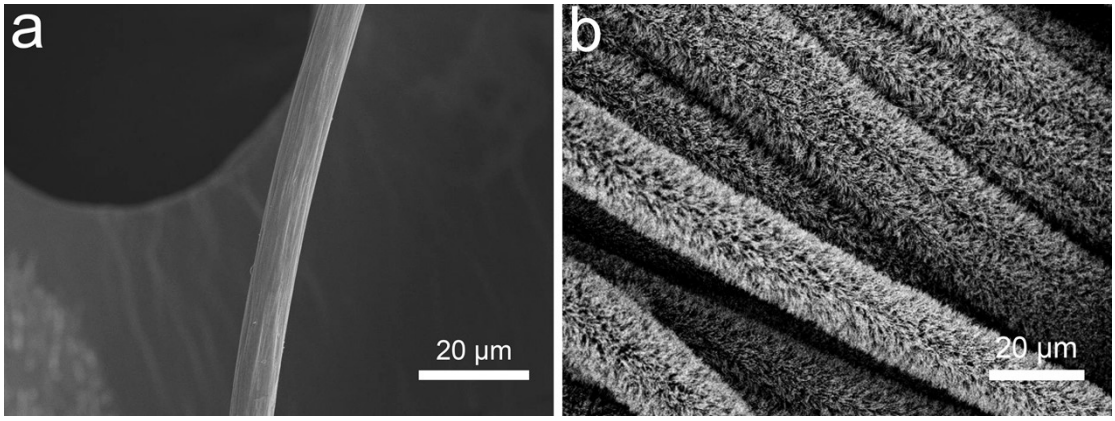

Fig. S1. SEM images of (a) bare CC and (b) $FeCo_2O_4$/CC.

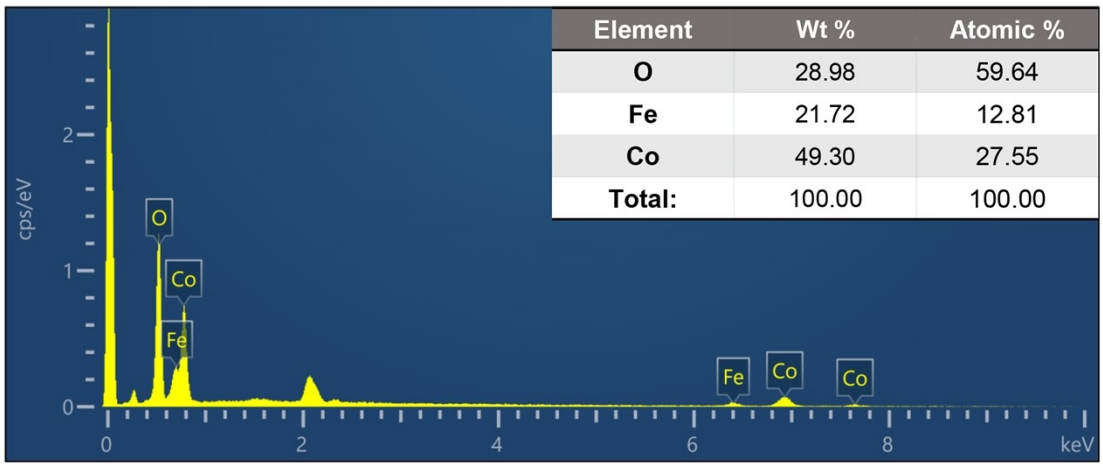

Fig. S2. EDX spectrum of $FeCo_2O_4$/CC.

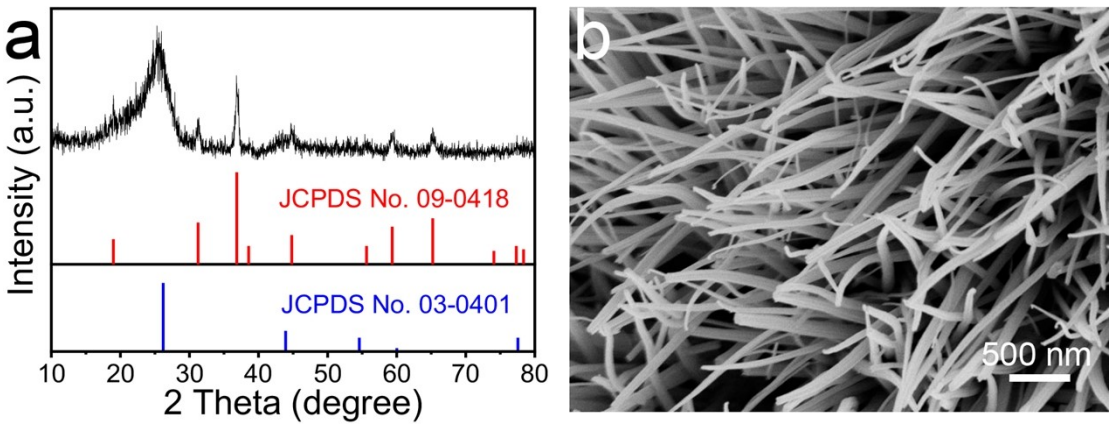

Fig. S3. (a) XRD pattern and (b) SEM image of Co_3O_4/CC.

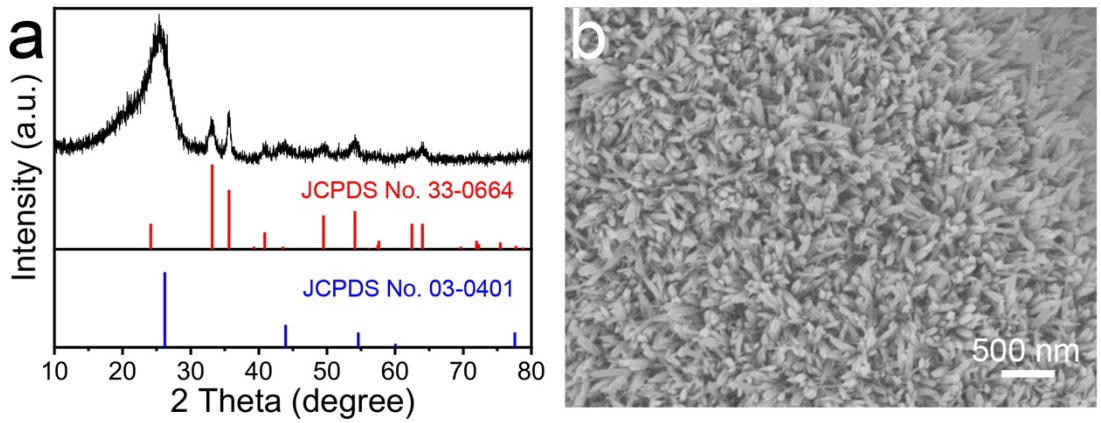

Fig. S4. (a) XRD pattern and (b) SEM image of Fe_2O_3/CC.

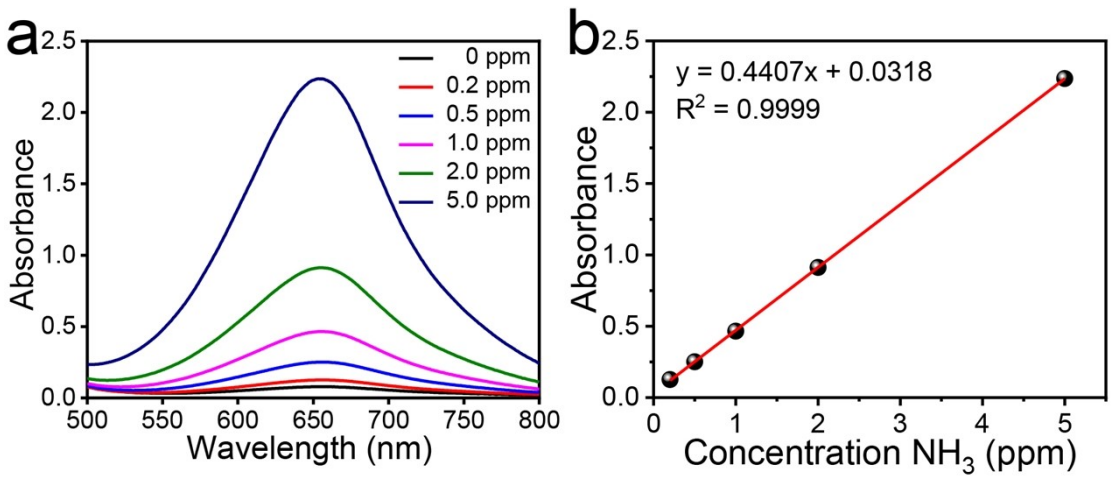

Fig. S5. (a) UV-Vis absorption spectra of indophenol assays kept with different concentrations of NH_4^+ after incubated for 2 h at room temperature. (b) Calibration curve used for estimation of NH_4^+ concentration.

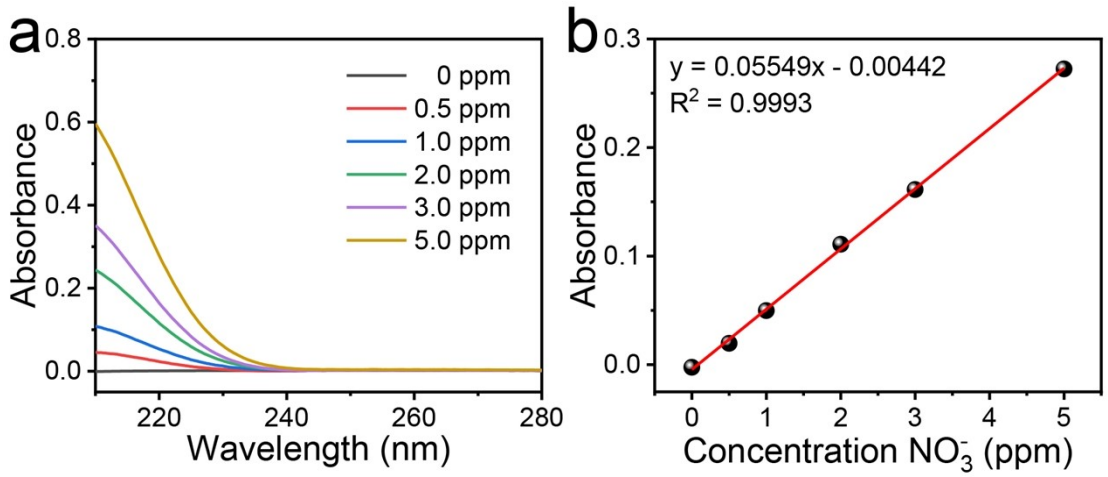

Fig. S6. UV-Vis absorption spectra of various NO_3^- concentrations after incubated for 15 min at room temperature. (b) Calibration curve used for calculation of NO_3^- concentration.

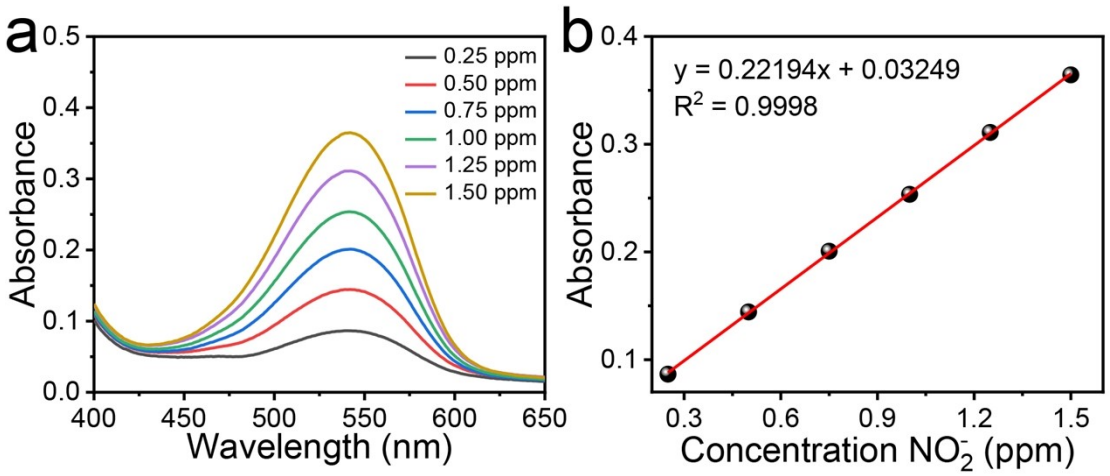

Fig. S7. UV-Vis absorption spectra of various NO_2^- concentrations after incubated for 10 min at room temperature. (b) Calibration curve used for quantification of NO_2^- concentration.

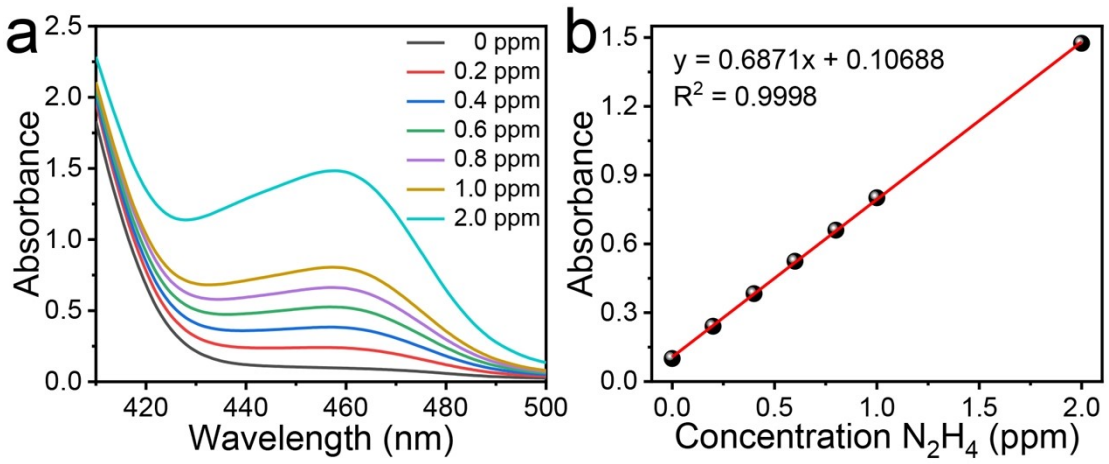

Fig. S8. (a) UV-Vis absorption spectra of various N_2H_4 concentrations after incubated for 15 min at room temperature. (b) Calibration curve used for calculation of N_2H_4 concentration.

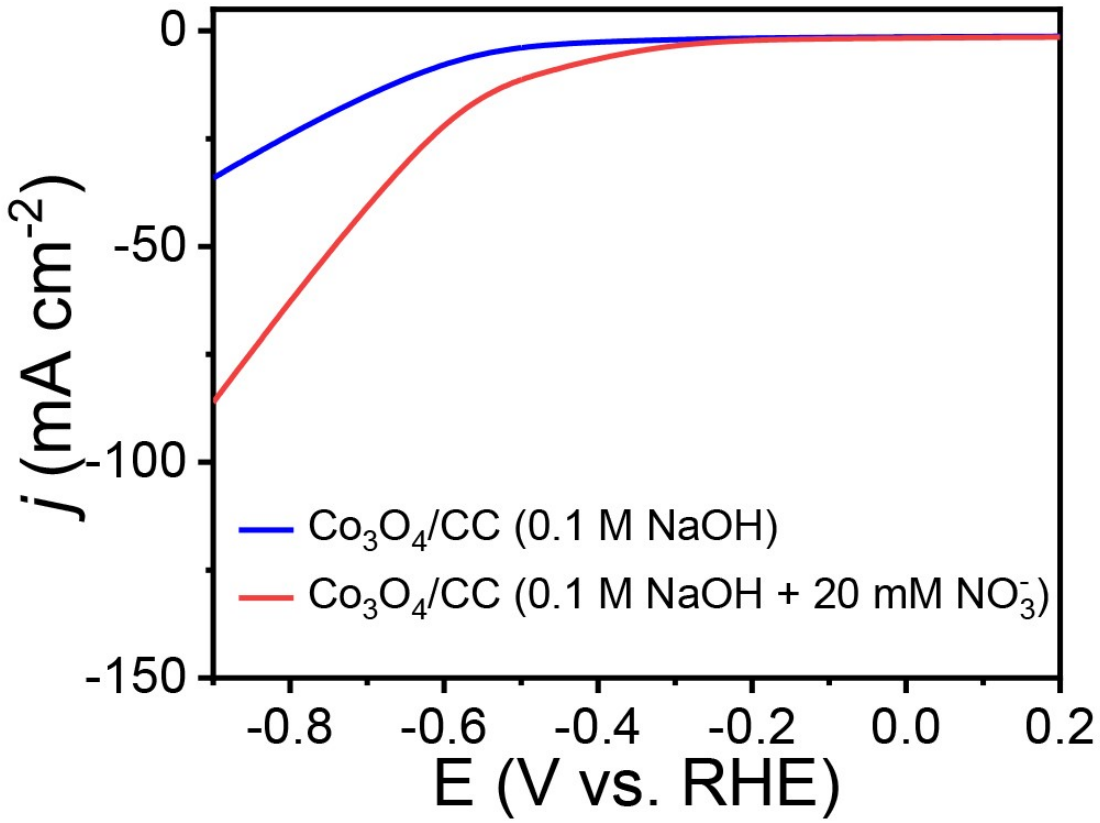

Fig. S9. LSV curves of Co_3O_4/CC in 0.1 M NaOH with and without 20 mM NO_3^-.

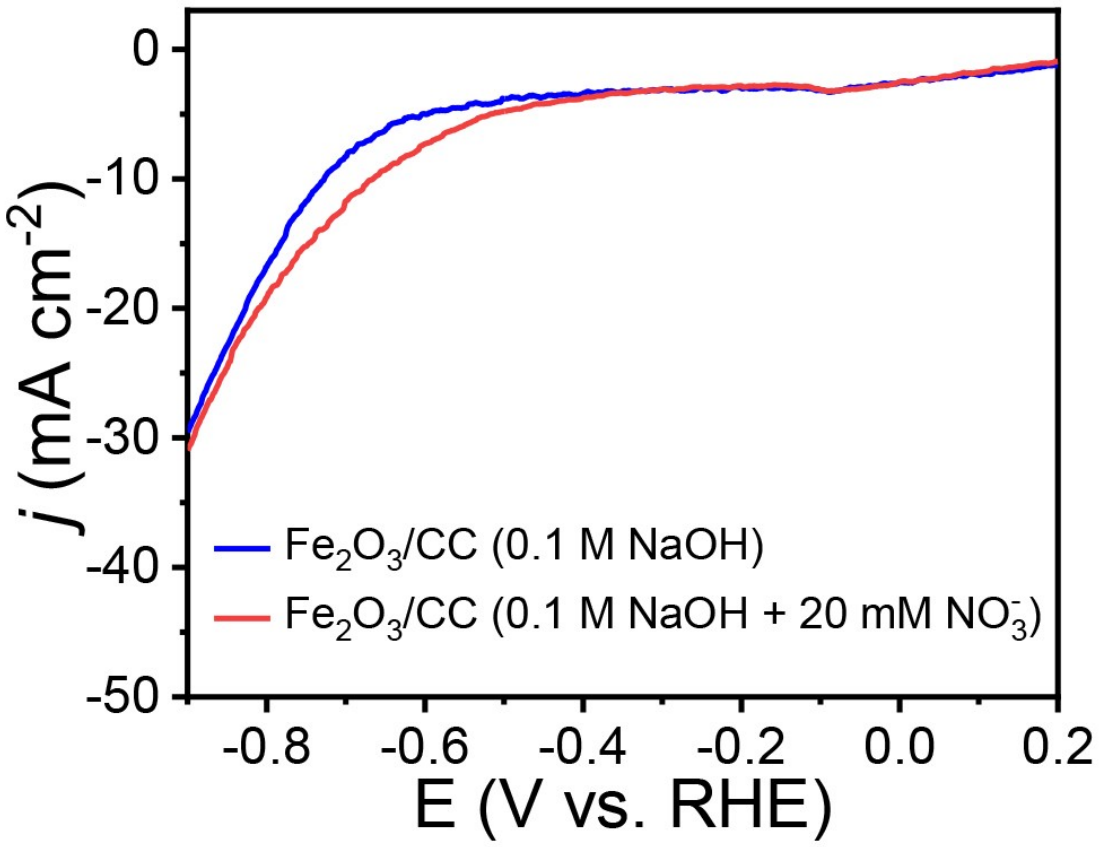

Fig. S10. LSV curves of Fe_2O_3/CC in 0.1 M NaOH with and without 20 mM NO_3^-.

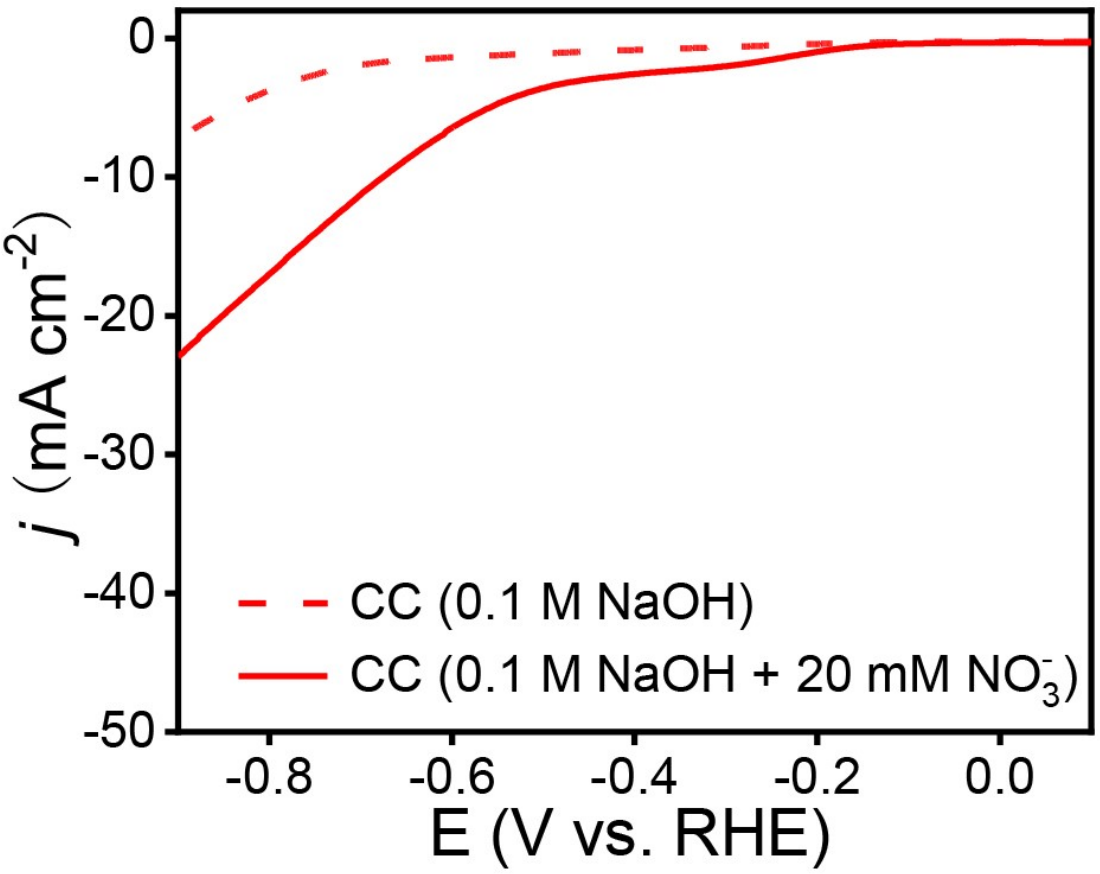

Fig. S11. LSV curves of bare CC in 0.1 M NaOH with and without 20 mM NO_3^-.

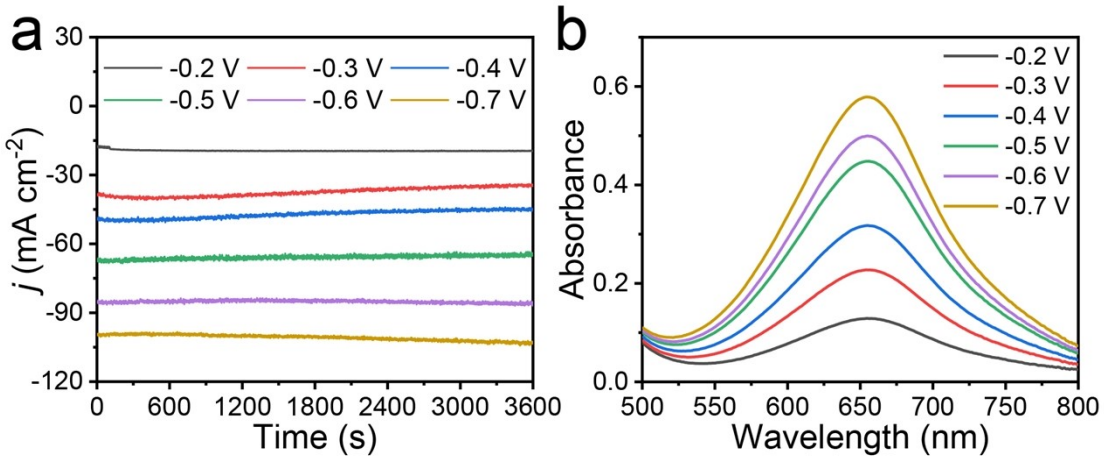

Fig. S12. (a) Chronoamperometry curves and (b) corresponding UV-Vis absorption spectra.

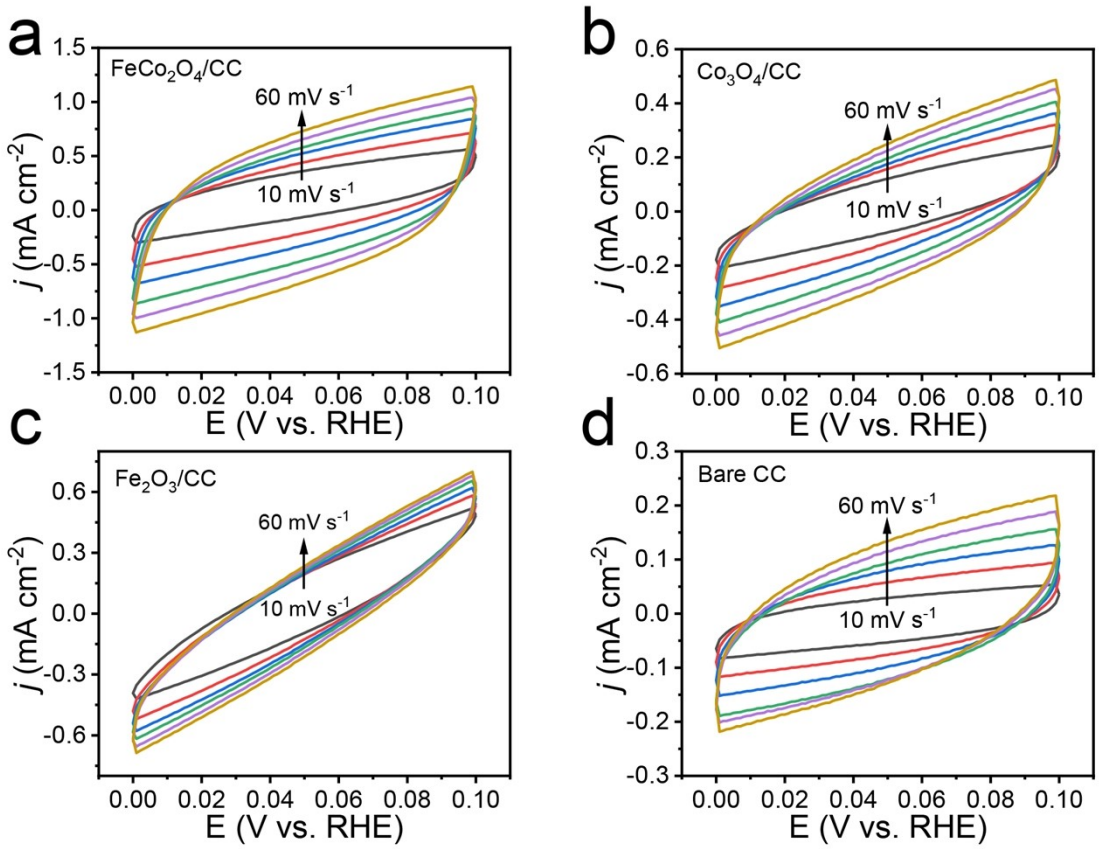

Fig. S13. CV curves of (a) $FeCo_2O_4$/CC, (b) Co_3O_4/CC, (c) Fe_2O_3/CC and (d) bare CC recorded in the non-Faradaic region of 0–0.1 V at various scan rates (10–60 mV s^{-1}). The electrochemical double-layer capacitances (C_{dl}) are the slopes of the linear fits.

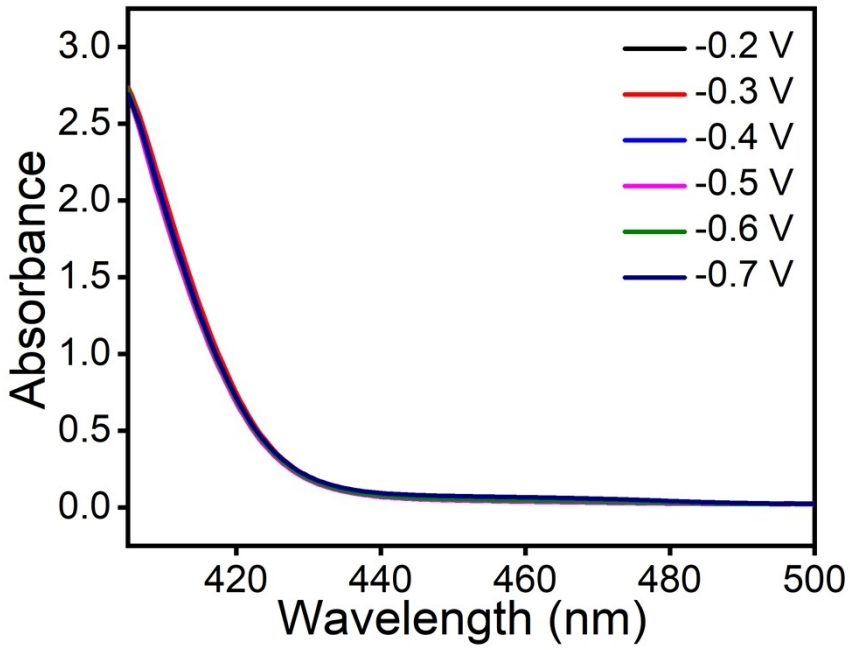

Fig. S14. UV-Vis absorption spectra of the electrolytes estimated by the method of Watt and Chrisp for the calculation of N_2H_4 concentration.

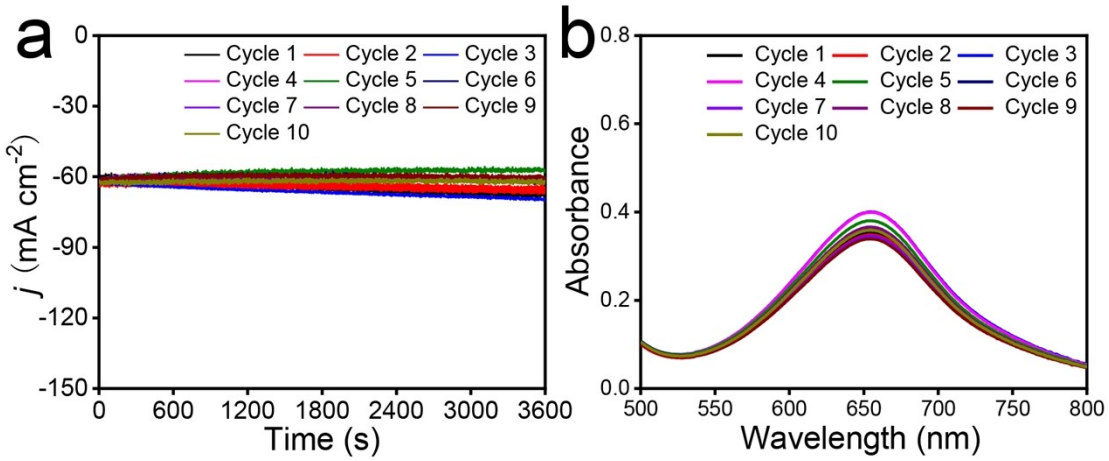

Fig. S15. (a) Chronoamperometry curves and (b) corresponding UV-Vis absorption spectra of $FeCo_2O_4$/CC for electrogenerated NH_3 during recycling tests at –0.5 V.

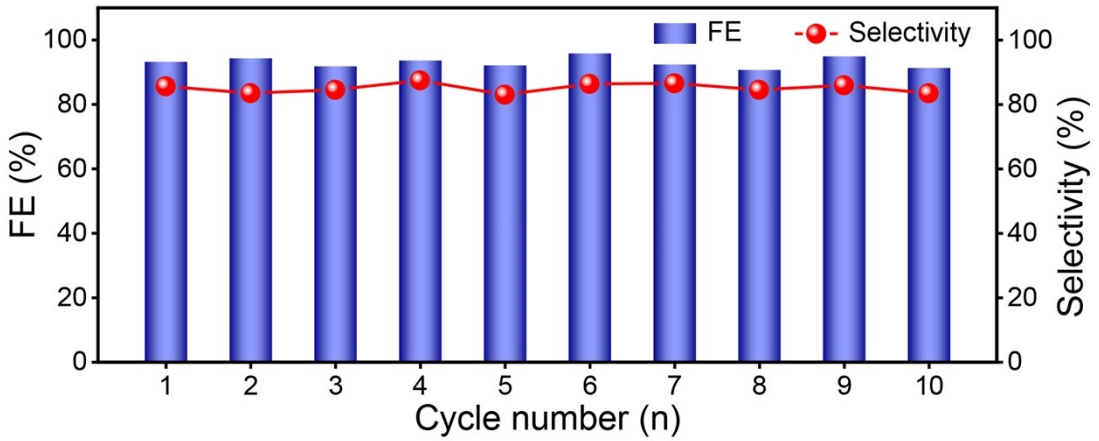

Fig. S16. Selectivity and FEs for NH_3 during recycling test at –0.5 V.

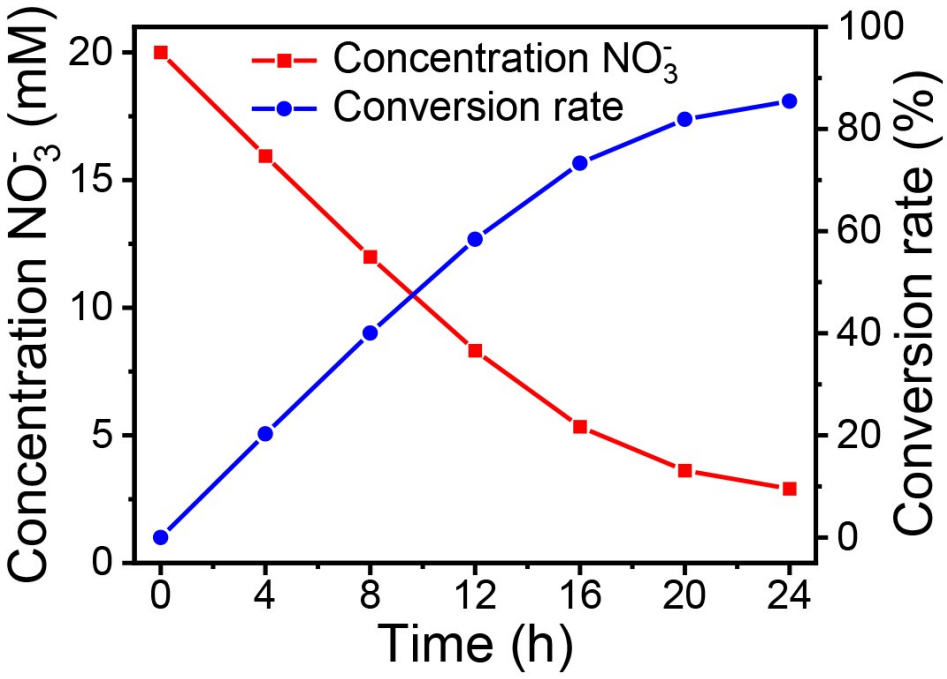

Fig. S17. Conversion rates and concentrations of NO_3^- during 24-h electrolysis at –0.5 V.

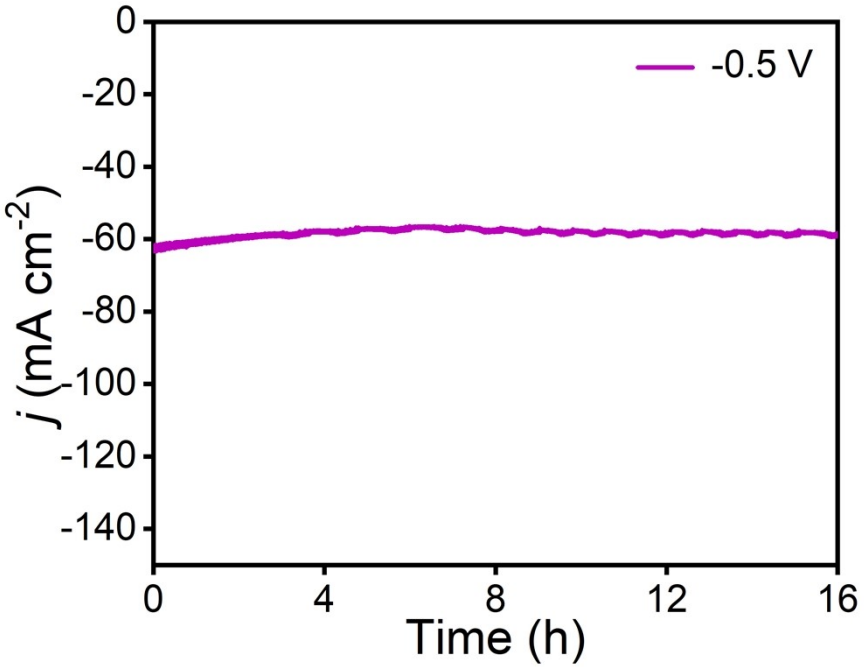

Fig. S18. Chronoamperometry curve of $FeCo_2O_4$/CC at −0.5 V for 16 h.

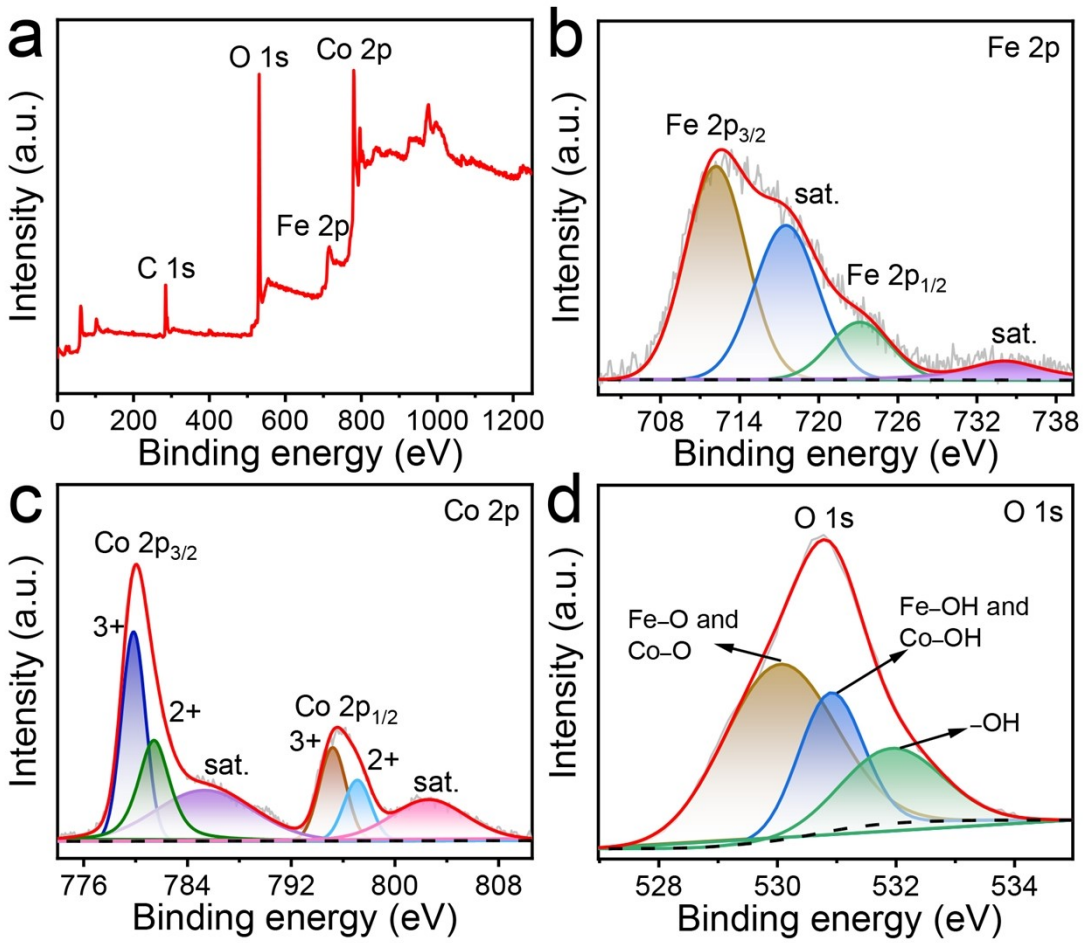

Fig. S19. (a) XPS survey spectrum for post-test $FeCo_2O_4$/CC. High-resolution XPS spectra of (b) Fe 2p, (c) Co 2p and (d) O 1s.

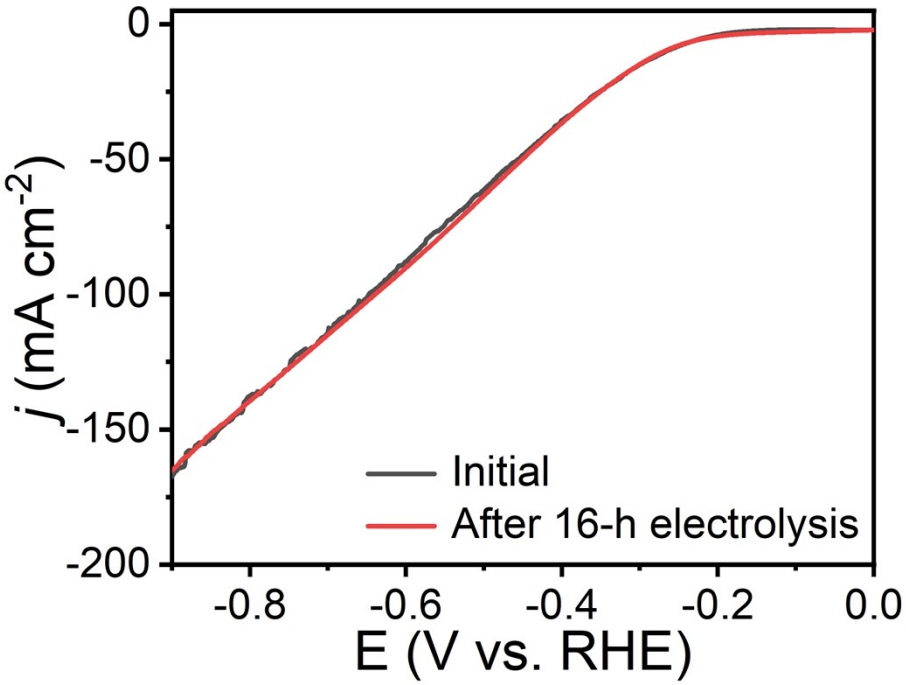

Fig. S20. LSV curves of $FeCo_2O_4$/CC before and after 16-h electrolysis.

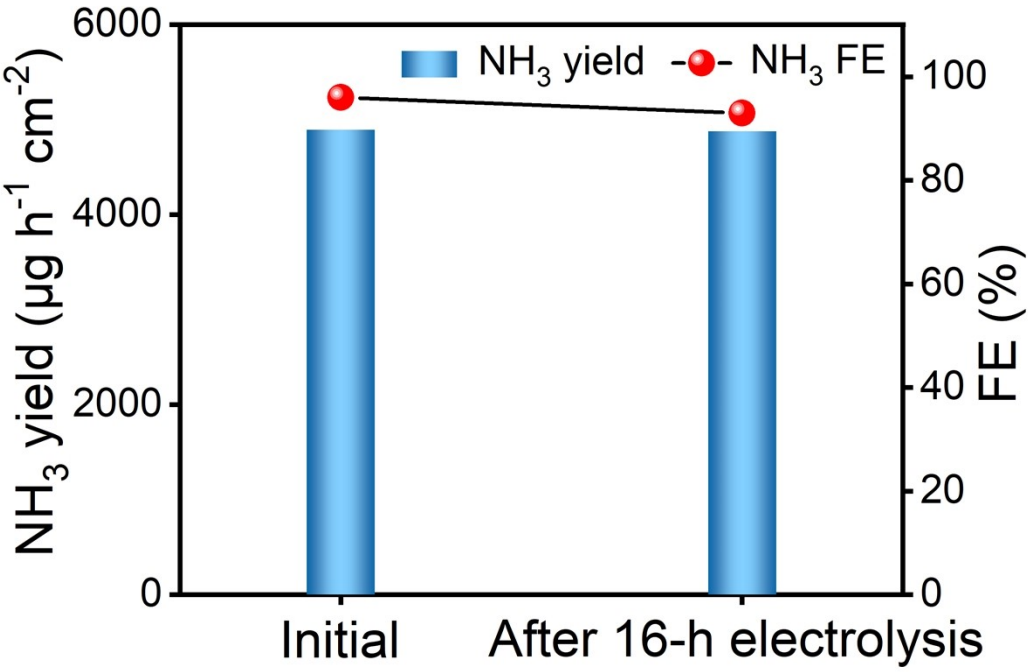

Fig. S21. NH_3 yields and FEs of $FeCo_2O_4$/CC before and after 16-h electrolysis.

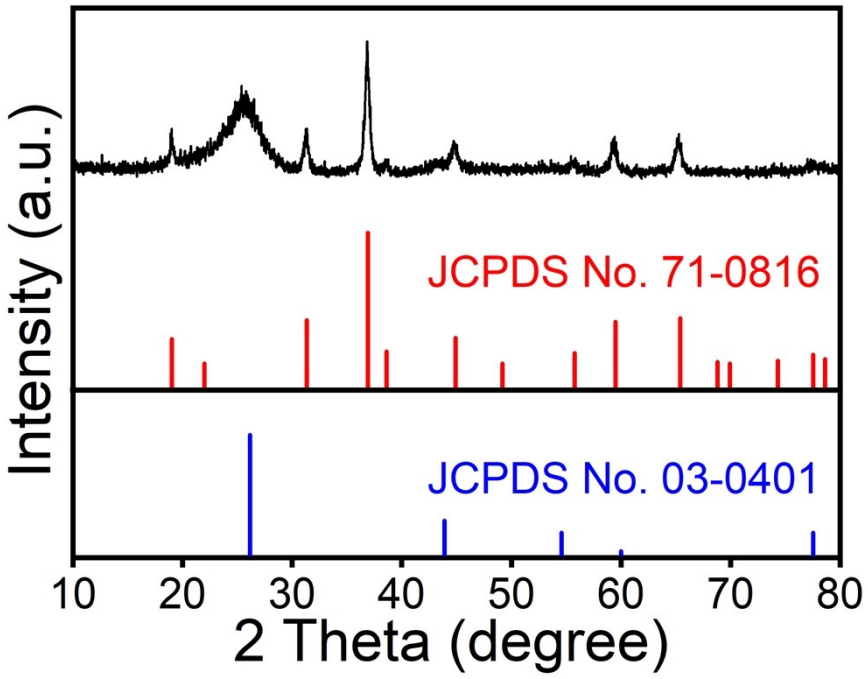

Fig. S22. XRD pattern of $FeCo_2O_4$/CC after 16-h electrolysis.

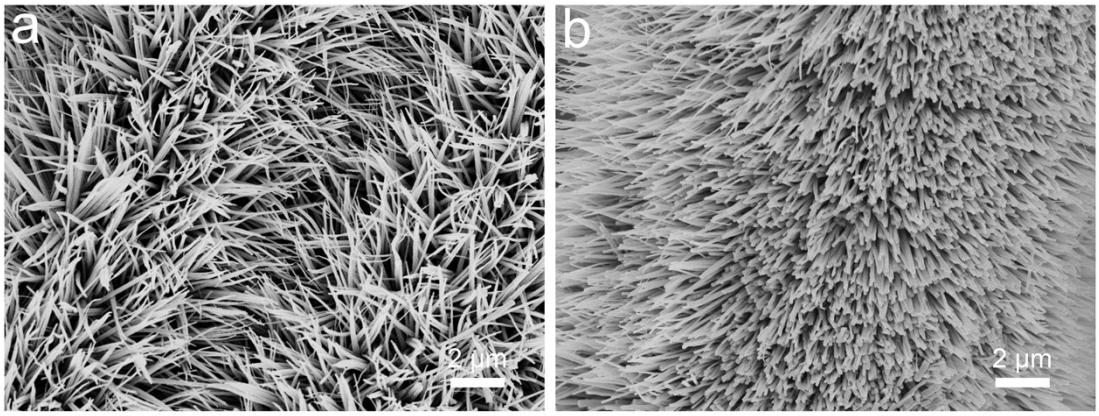

Fig. S23. SEM images of $FeCo_2O_4$/CC (a) before and (b) after 16-h electrolysis.

Table S1. Comparison of catalytic performance of $FeCo_2O_4$/CC with other reported NO_3RR electrocatalysts.

Catalyst	Electrolyte	NH_3 yield@Potential (V vs. RHE)	FE@Potential (V vs. RHE)	Ref.
$FeCo_2O_4$/CC	0.1 M NaOH (20 mM NO_3^-)	4988 μg h^{-1} cm^{-2}@–0.5	95.9%@–0.5	This work
Pd facets	0.1 M NaOH (20 mM NO_3^-)	306.8 μg h^{-1} cm^{-2}@–0.2	35%@–0.2	3
Ni NP	1 M NaOH (20 mM NO_3^-)	/	46.3%@–0.27	4
Pd/TiO_2	0.5 M NaOH (250 mM NO_3^-)	1120 μg h^{-1} cm^{-2}@–0.7	92%@–0.7	5
Cu	1 M NaOH (0.1 M NO_3^-)	/	79%	6
In–S–G	1 M KOH (100 mM NO_3^-)	3740 μg h^{-1} $mg_{cat.}^{-1}$@–0.5	75%@–0.5	7
Fe SAC	1 M KOH (100 mM NO_3^-)	/	86%@–0.21	8
CuNiCe alloy	0.5 M KOH (50 mM NO_3^-)	/	90%@–0.3	9
BC_2N/Pd	0.1 M KOH (250 mM NO_3^-)	1730 μg h^{-1} cm^{-2}@–0.7	97.42%@–0.3	10
Fe–PPy SACs	0.1 M KOH (100 mM NO_3^-)	2750 μg h^{-1} cm^{-2}@–0.7	~100%@–0.3	11
BCN@Ni	0.1 M KOH (100 mM NO_3^-)	2320.2 μg h^{-1} cm^{-2}@–0.5	91.15%@–0.3	12
Ni_3B@$NiB_{2.74}$	0.1 M KOH (100 mM NO_3^-)	3371.1 μg h^{-1} cm^{-2}@–0.3	~100%@–0.3	13
BCN-Cu	0.1 M KOH (100 mM NO_3^-)	1900.07 μg h^{-1} cm^{-2}@–0.5	98.23%@–0.5	14
$ZnCo_2O_4$	0.1 M KOH (100 mM NO_3^-)	2101.2 μg h^{-1} $mg_{cat.}^{-1}$@–0.6	95.4%@–0.4	15
Cu nanosheets	0.1 M KOH (10 mM NO_3^-)	390.1 μg h^{-1} $mg_{cat.}^{-1}$@–0.15	99.7%@–0.15	16
$Cu_{50}Ni_{50}$	1 M KOH (10 mM NO_3^-)	/	84 ± 2%	17

References

1 D. Zhu, L. Zhang, R. E. Ruther and R. J. Hamers, *Nat. Mater.,* 2013, **12**, 836–841.

2 G. W. Watt and J. D. Chrisp, *Anal. Chem.,* 1952, **24**, 2006–2008.

3 J. Lim, C. Liu, J. Park, Y. Liu, T. P. Senftle, S. W. Lee and M. C. Hatzell, *ACS Catal.,* 2021, **11**, 7568–7577.

4 L. Mattarozzi, S. Cattarin, N. Comisso, P. Guerriero, M. Musiani, L. Vázquez-Gómez and E. Verlato, *Electrochim. Acta*, 2013, **89**, 488–496.

5 Y. Guo, R. Zhang, S. Zhang, Y. Zhao, Q. Yang, Z. Huang, B. Dong and C. Zhi, *Energy Environ. Sci.,* 2021, **14**, 3938–3944.

6 D. Reyter, G. Chamoulaud, D. Bélanger and L. Roué, *J. Electroanal. Chem.,* 2006, **596**, 13–24.

7 F. Lei, W. Xu, J. Yu, K. Li, J. Xie, P. Hao, G. Cui and B. Tang, *Chem. Eng. J.,* 2021, **426**, 131317.

8 Z. Wu, M. Karamad, X. Yong, Q. Huang, D. A. Cullen, P. Zhu, C. Xia, Q. Xiao, M. Shakouri, F. Chen, J. Y. Kim, Y. Xia, K. Heck, Y. Hu, M. S. Wong, Q. Li, I. Gates, S. Siahrostami and H. Wang, *Nat. Commun.*, 2021, **12**, 2870.

9 C. Lu, S. Lu, W. Qiu and Q. Liu, *Electrochim. Acta*, 1999, **52**, 2193–2197.

10 X. Li, X. Zhao, Y. Zhou, J. Hu, H. Zhang, X. Hu and G. Hu, *Appl. Surf. Sci.*, 2022, **584**, 152556.

11 P. Li, Z. Jin, Z. Fang and G. Yu, *Energy Environ. Sci.*, 2021, **14**, 3522–3531.

12 X. Zhao, Z. Zhu, Y. He, H. Zhang, X. Zhou, W. Hu, M. Li, S. Zhang, Y. Dong, X. Hu, A. V. Kuklin, G. V. Baryshnikov, H. Ågren, T. Wågberg and G. Hu, *Chem. Eng. J.*, 2022, **433**, 133190.

13 L. Li, C. Tang, X. Cui, Y. Zheng, X. Wang, H. Xu, S. Zhang, T. Shao, K. Davey and S. Qiao, *Angew. Chem., Int. Ed.*, 2021, **60**, 14131–14137.

14 X. Zhao, X. Jia, Y. He, H. Zhang, X. Zhou, H. Zhang, S. Zhang, Y. Dong, X. Hu, A. V. Kuklin, G. V. Baryshnikov, H. Ågren and G. Hu, *Appl. Mater. Today*, 2021, **25**, 101206.

15 P. Huang, T. Fan, X. Ma, J. Zhang, Z. Chen and X. Yi, *ChemSusChem*, 2022, DOI: 10.1002/cssc.202102049.

16 X. Fu, X. Zhao, X. Hu, K. He, Y. Yu, T. Li, Q. Tu, X. Qian, Q. Yue, M. R. Wasielewski and Y. Kang, *Appl. Mater. Today*, 2020, **19**, 100620.

17 Y. Wang, A. Xu, Z. Wang, L. Huang, J. Li, F. Li, J. Wicks, M. Luo, D. H. Nam, C. Tan, Y. Ding, J. Wu, Y. Lum, C. T. Dinh, D. Sinton, G. Zheng and E. H. Sargent, *J. Am. Chem. Soc.,* 2020, **142**, 5702–5708.